Semiclassically modeling Hydrogen at Rydberg states immersed in electromagnetic fields

Jaron Williams and Dr. John Shaw

Louisiana Tech University

(Dated: May 20, 2019)

Abstract

Originally, closed-orbit theory was developed in order to analyze oscillations in the near ionization threshold (Rydberg) densities of states for atoms in strong external electric and magnetic fields. Oscillations in the density of states were ascribed to classical orbits that began and ended near the atom. In essence, observed outgoing waves following the classical path return and interfere with original outgoing waves, giving rise to oscillations. Elastic scattering from one closed orbit to another gives additional oscillations in the cross-section. This study examines how quantum theory can be properly used in combination with classical orbit theory in order to study inelastic scattering for atoms in an external field. At Rydberg states, an electron wave function can be modeled numerically through semiclassical means, using the Coulombic interaction from the atom, but as it approaches lower states, it must be modeled quantum mechanically, using a 'Modified Coulombic' potential.

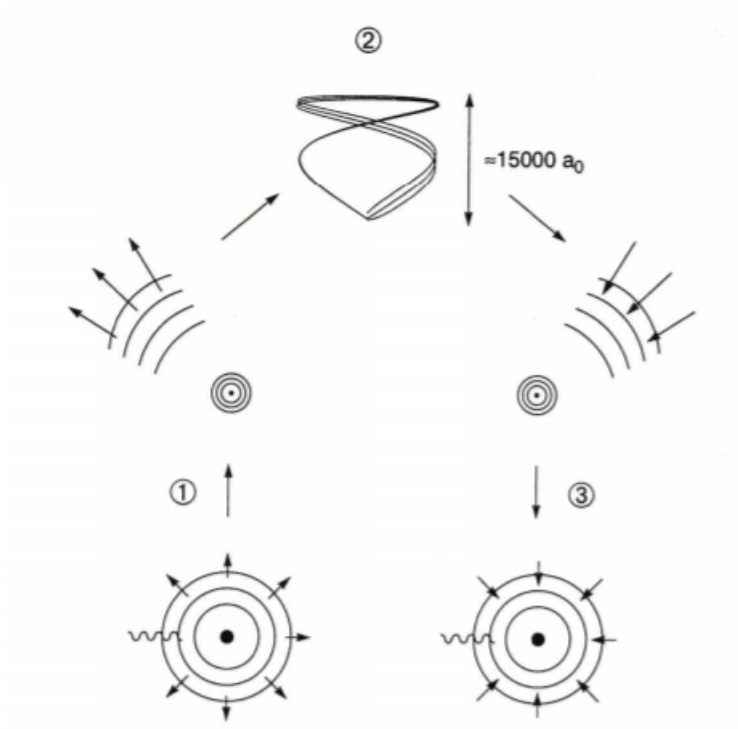

FIG. 1: A sketch illustrating the theory of how a Rydberg atom behaves in a magnetic field.

INTRODUCTION

In 1969, Garton and Tomkins studied the excited states of Barium in a magnetic field. At lower energies, the structure of the spectrum is determined relatively easily as linear. However, as energy is increased, oscillations begin to occur and a sinusoidal behavior arises in the probability of absorption. Effects of an external magnetic field continue to add complexities, and remain unsolved. One positive to this model: most atoms in Rydberg states can be modeled similarly to Hydrogen, simplifying the process immensely. In an atom, if a photon with the right energy hits a valence electron, it will be sent up to higher energy states, and in some cases be ionized. However, the electron can also be sent to a near-ionization state, known as a Rydberg state. At such a state, the electron still does not have sufficient energy to escape the potential well of the atom. This lack of energy results in a classical orbit that comes back to the nucleus of the atom.

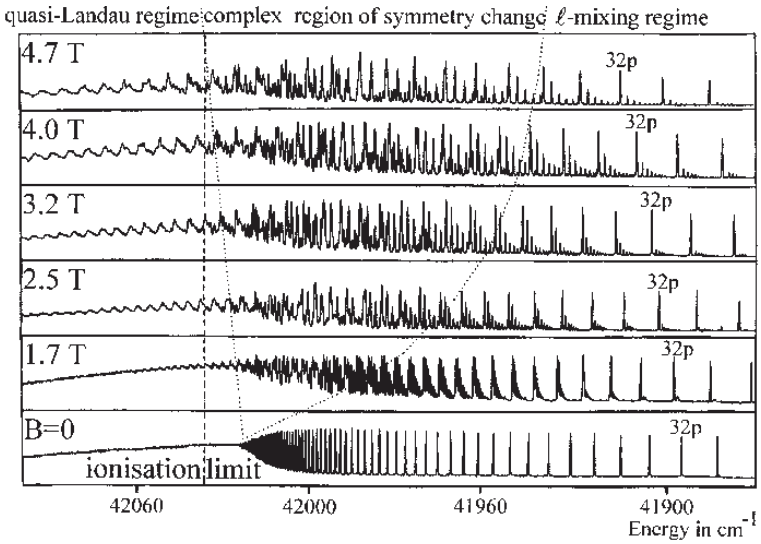

FIG. 2: The absorption spectrum of Barium in a magnetic field.

METHODS

Using a predetermined outgoing wave function determined from a purely quantum mechanical calculation, we can determine the returning wave semiclassically:

$$\Psi_{ret}(\vec{q}) = \int G(\vec{q},\vec{q}';E)\Psi_{out}(\vec{q}')d\vec{q}' \tag{1}$$

Where G is a Green's function operating on Ψ_{out}, and gives a complex Ψ_{ret} we can write as:

$$\Psi_{ret} = Ae^{iS} \tag{2}$$

The density of states can be shown as:

$$\sigma = \sigma_0 + \sigma_{osc} \tag{3}$$

Where the oscillatory part is represented as the imaginary overlap of the returning and outgoing wave functions:

$$\sigma_{osc} \propto Im < \Psi_{ret}|\Psi_{out} > \tag{4}$$

$$\propto \Sigma_k A_k(\vec{q},\vec{q}')sin(S_k(\vec{q},\vec{q}') + \mu_k\frac{\pi}{2}) \tag{5}$$

The amplitude depends on the stability matrix J and S on the kth classical path. $J_{21} \to 0$ at bifurcations of an orbit unless higher order terms included in A and S.

$$A_k = \frac{1}{|J_{21}|^{1/2}} = \frac{1}{|\frac{\partial^2 \tilde{S}}{\partial v^2}|^{1/2}} \qquad S_k = \int \vec{p_q} d\vec{q}$$

The system hamiltonian can be represented by:

$$H = \frac{p^2}{2} - \frac{1}{\rho} + \frac{1}{2} L_z B + \frac{1}{8} B^2 \rho^2 \tag{6}$$

This system is not separable in any orthogonal coordinate system, so it must be solved via perturbation theory.

The new Semiparabolic coordinate system is described as:

$$\rho = uv \tag{7}$$

$$z = \frac{(u^2 - v^2)}{2} \tag{8}$$

$$p_\rho = \frac{1}{u^2 + v^2}(v p_u + u p_v) \tag{9}$$

$$p_z = \frac{1}{u^2 + v^2}(u p_u - v p_v) \tag{10}$$

The new coordinate system gives rise to a new Hamiltonian:

$$h = (u^2 + v^2)(H - E) + 2 \tag{11}$$

Which, when expanded, is seen as:

$$h = \frac{p_u^2}{2} + \frac{p_v^2}{2} + \frac{1}{8} B^2 u^2 v^2 (u^2 + v^2) \tag{12}$$
$$+ \frac{1}{2} F(u^4 - v^4) - E(u^2 + v^2) = 2$$

The phase space is a planar slice of the 4-D system, plotting p_v against v at the $u = 0$ surface.

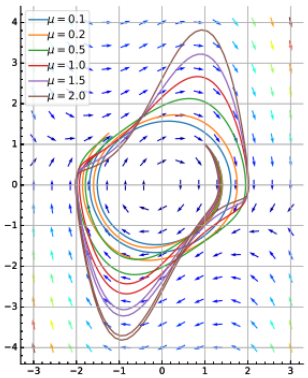

FIG. 3: An example of a phase space portrait.

The linearized dynamics on the Poincaré map is given by the Jacobian matrix:

$$J(j) = \begin{pmatrix} \frac{\partial q_f}{\partial q_i} & \frac{\partial q_f}{\partial p_{q,i}} \\ \frac{\partial p_{q,f}}{\partial q_i} & \frac{\partial p_{q,f}}{\partial p_{q,i}} \end{pmatrix} = \begin{pmatrix} J_{11} & J_{12} \\ J_{21} & J_{22} \end{pmatrix} \tag{13}$$

The mapping preserves area, so $det(J) = 1$, and the eigenvalues are complex when $|Tr(J(j))| < 2$, and purely real when $|Tr(J(j))| > 2$. Thus, when $|Tr(J(j))| > 2$, $J_{12}(j)$ grows exponentially, and the orbit becomes unstable.

The properties of J encode the dynamics of the linear system:

$$\text{If } \vec{q} = (u, v, p_u, p_v) \text{ such that } \frac{d\vec{q}}{dt} = J\,\vec{q} + \Omega_{NL}$$

Neglecting the nonlinear terms, we get solutions that look like:

$$\vec{q} = e^{\vec{\lambda} t}, \text{ with a diagonalized } J = \begin{pmatrix} \lambda_1 & 0 \\ 0 & \lambda_2 \end{pmatrix}$$

Then, for $\lambda \in \mathbb{C}$, $\lambda = \alpha + i\beta$. So, if $\alpha = 0$, we have oscillatory motion, and if $\beta = 0$, we have instability.

Bifurcation theory is used to analyze how a dynamical system changes with respect to a varying parameter - where and when fixed points arise and disappear. A pitchfork bifurcation occurs when a pair of fixed points appears/disappears symmetrically.

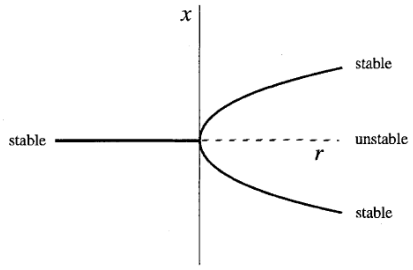

FIG. 4: A pitchfork bifurcation, varied by a parameter r.

Strogatz

Theoretical mappings of systems of this form look like: The Hartman-Grobman Theorem states that in a neighborhood around a hyperbolic fixed point, the phase space of a dynamical system is homeomorphic to another of the same form.From this, we can approximate the

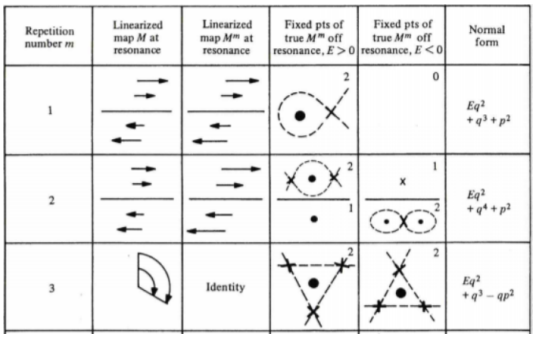

FIG. 5: A chart of normal forms.

dynamics of a nonlinear system near its fixed points. Furthermore, we can draw parallels between two dynamical systems that share the same form.

Since the Hamiltonian cannot be separated in any coordinate system, it must be dealt with numerically.The numerical integrator uses a fourth order Runge-Kutta method to solve the system.

Recall:

$$\sigma_{osc} = \Sigma_k A_k(\vec{q},\vec{q}')sin(S_k(\vec{q},\vec{q}') + \mu_k\frac{\pi}{2}) \tag{14}$$

The calculations of A_k, S_k, and μ_k involve classical paths. The equations of motion as shown are integrated, which becomes a summation of the classical orbits, giving the density of states.

CONCLUSION

The trace, as varied with scaled energy is shown in Figure 6. The phase space is shown in Figures 8-23.

It is seen that the dynamical system modeled mirrors that of the expected normal form, and thus, through time, satisfies the Hartman-Grobman Theorem near the origin. Near the fixed points are points at $v = 0$, in the neighborhood of the surface of section $u \to 0$. In order to fit the Hamiltonian to a normal form, we define a canonical transformation $H(u, \frac{-\partial\tilde{S}}{\partial p_v}, \frac{\partial\tilde{S}}{\partial u}, p_v)$

Such that $\tilde{S}(u, p_v)$, and:

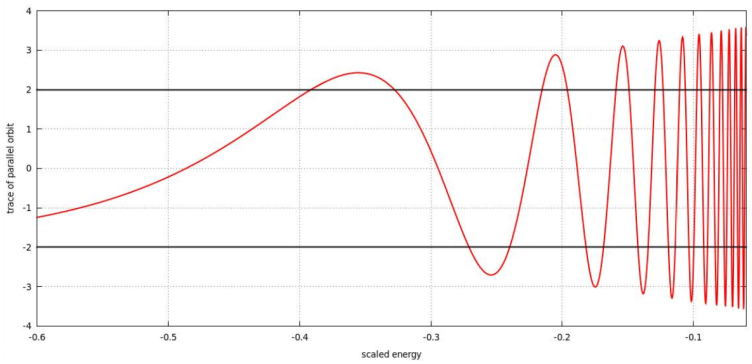

FIG. 6: Trace plotted against scaled energy.

$$v = \frac{-\partial \tilde{S}}{\partial p_v} \qquad\qquad p_u = \frac{\partial \tilde{S}}{\partial u}$$

For orbits along the p_v axis in a B-field,

$$\tilde{S} = u\sqrt{2E - p_v^2} + F(p_v) \tag{15}$$

Where:

$$F(p_v) = \sum_n \frac{a_{2n}}{2n} p_v^{2n}, n \in \mathbb{N}$$

We approximate using our quartic terms:

$$F(p_v) = \frac{a_2}{2} p_v^2 + \frac{a_4}{4} p_v^4 \tag{16}$$

We can rewrite $F(p_v)$ as:

$$F(p_v) = \frac{a_4}{4}\left(\frac{2a_2}{a_4} p_v^2 + p_v^4\right) \tag{17}$$

And re-parameterize, such that $\lambda := \frac{2a_2}{a_4}$, then for $\lambda \in \{-1, -.5, 0, .5, 1\}$, F takes the form:

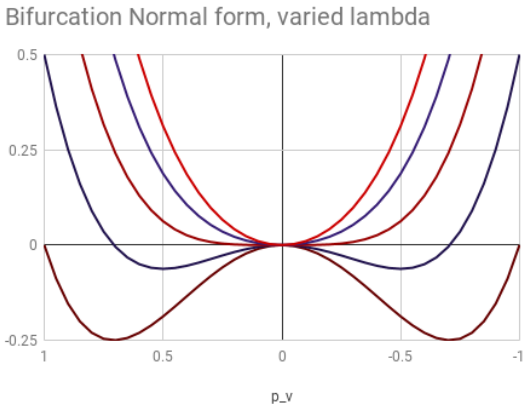

FIG. 7: Bifurcation as λ is varied.

The final returning wave function is represented as:

$$\Psi_{ret} = Ae^{i\tilde{S}} \tag{18}$$

Which is including the nonlinearities, resulting in a lack of singularity in Ψ_{ret}, since $A_k \nrightarrow \infty$ as $J_{21} \to 0$ in the nonlinear approximation to the kth orbit.

Therefore, we have a successful way to numerically integrate the returning wavefunctions of the Rydberg Hydrogen atom in a magnetic field.

BIBLIOGRAPHY

[1] David J. Griffiths. *Introduction to Quantum Mechanics*. Prentice Hall, Inc. New Jersey, 1995.

[2] Matthias Brack, Rajat K. Bhaduri. *Semiclassical Physics*. Addison Wesley Publishing Company, Massachusetts, 1997.

[3] Steven H. Strogatz. *Nonlinear Dynamics and Chaos*. Westview Press, Colorado, 1997.

[4] J.-M. Mao, J.B. Delos *Hamiltonian bifurcation theory of closed orbits in the diamagnetic Kepler problem*. Physical Review A, 1992.

[5] T. van der Veldt. *Diamagnetism in Helium Rydberg atoms*. Febodruk, 1993.

[6] Michael Courtney *Rydberg atoms in strong fields: A testing ground for quantum chaos*. Massachusetts Institute of Technology, 1995.

[7] Kees Karremans *Signatures of chaos in spectra of diamagnetic helium Rydberg atoms*. Febodruk, 1999.

[8] Thomas Bartsch *The hydrogen atom in an electric field and in crossed electric and magnetic fields: Closed orbit theory and semiclassical quantization*. Universitat Stuttgart, 2002.

[9] Alfredo M. Ozorio de Almeida *Hamiltonian Systems: Chaos and Quantization*. Cambridge University Press, 1988.

[10] David Park *Classical Dynamics and its Quantum Analogues*. Springer-Verlag Berlin Heidelberg, 1979.

APPENDIX

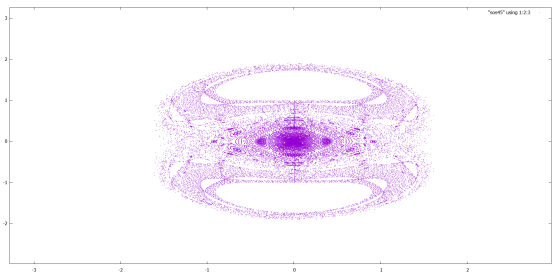

FIG. 8: $\epsilon = -.45$

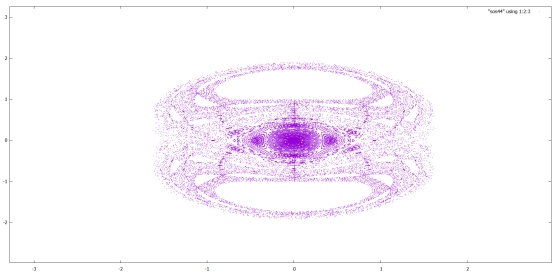

FIG. 9: $\epsilon = -.44$

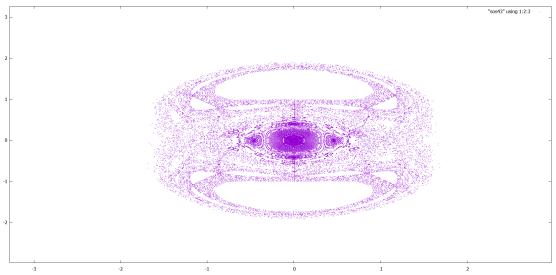

FIG. 10: $\epsilon = -.43$

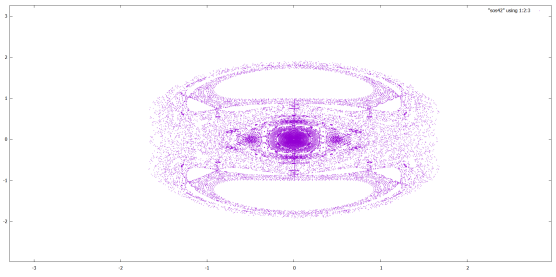

FIG. 11: $\epsilon = -.42$

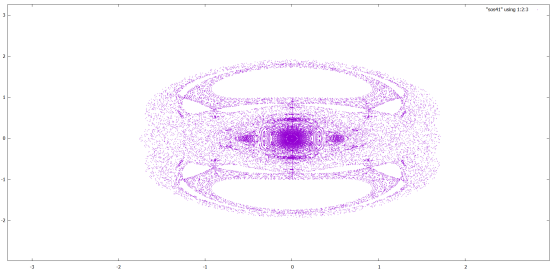

FIG. 12: $\epsilon = -.41$

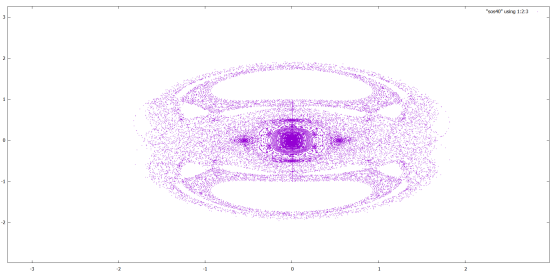

FIG. 13: $\epsilon = -.40$

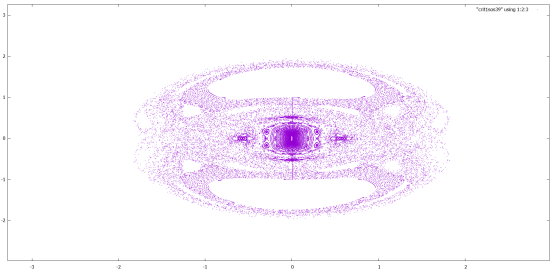

FIG. 14: $\epsilon = -.39$ (Critical Point)

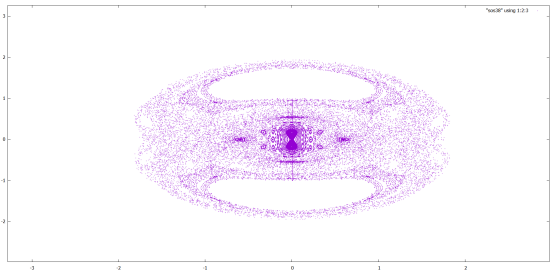

FIG. 15: $\epsilon = -.38$

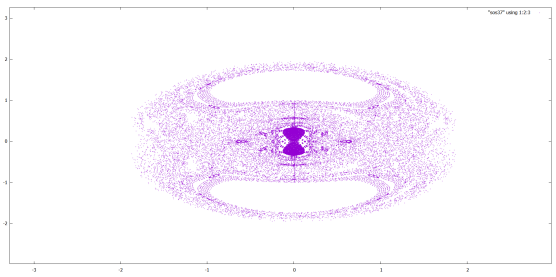

FIG. 16: $\epsilon = -.37$

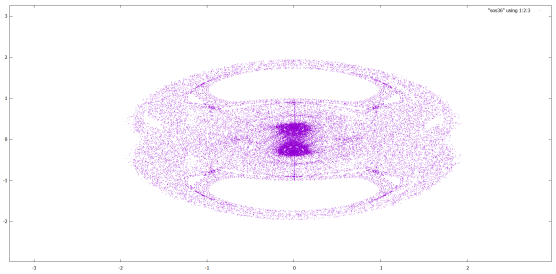

FIG. 17: $\epsilon = -.36$

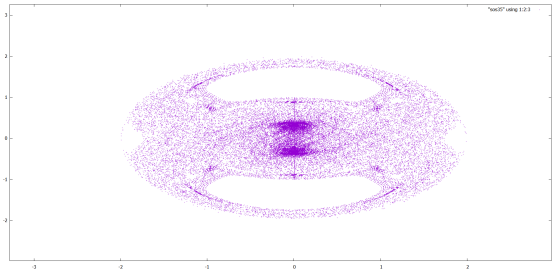

FIG. 18: $\epsilon = -.35$

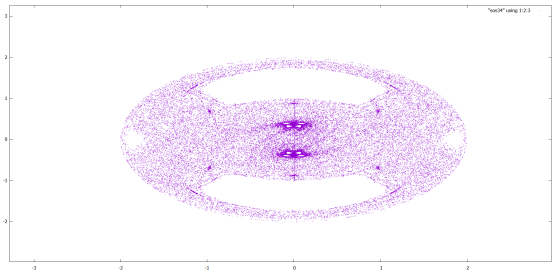

FIG. 19: $\epsilon = -.34$

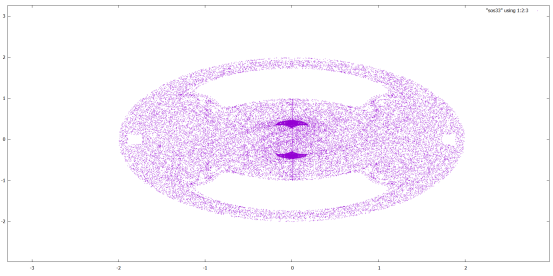

FIG. 20: $\epsilon = -.33$

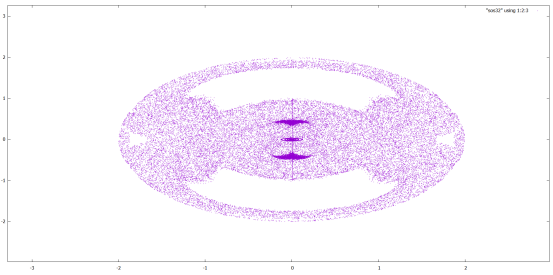

FIG. 21: $\epsilon = -.32$ (Critical Point)

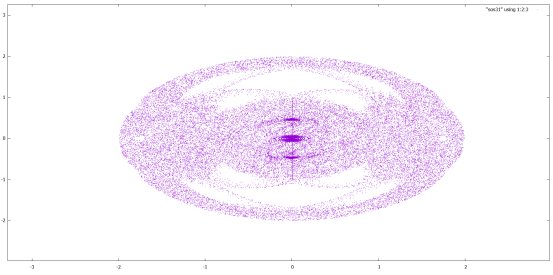

FIG. 22: $\epsilon = -.31$

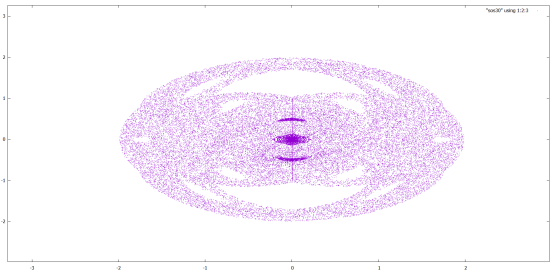

FIG. 23: $\epsilon = -.30$

FIG. 8-23: Phase space portraits of orbits at $u = 0$ surface of section.